DOI: 10.6060/ivkkt.20256812.7245

УДК: 544.778.4

ЭЛЕКТРОХИМИЧЕСКИЙ СИНТЕЗ ПРЕКУРСОРОВ ФЕРРИТОВ БАРИЯ С ИСПОЛЬЗОВАНИЕМ ВТОРИЧНОГО ТЕХНИЧЕСКОГО ЖЕЛЕЗА

А.Ф. Дресвянников, А.Э. Мухамадеев, А.И. Хайруллина, Э.Э. Валеева

Александр Федорович Дресвянников (ORCID 0000-0002-5824-2307)*, Артур Эдуардович Мухамадеев (ORCID 0009-0007-9222-8959), Алина Исмагиловна Хайруллина (ORCID 0000-0003-1683-3894), Эльвира Энверовна Валеева (ORCID 0000-0002-8376-0835)

Кафедра технологии электрохимических производств, Казанский национальный исследовательский технологический университет, ул. Карла Маркса, 68, Казань, Российская Федерация, 420015
E-mail: a.dresvyannikov@mail.ru*, m.artur_98@mail.ru, alina17xaj@mail.ru, elviravaleeva75@yandex.ru

В статье показана целесообразность использования анодного окисления низкоуглеродистой стали для получения ферритов бария. Во время электролиза раствор перемешивался за счет выделения водорода на катоде, а движение пузырьков газа обеспечивало перемещение масс электролита в направлении снизу вверх от центра к периферии, что способствует лучшему перемешиванию электрогенерируемых реагентов (OH^-, Fe^{2+}), компонентов электролита и уменьшению концентрационной поляризации. Согласно современным представлениям, на аноде происходит образование растворимых поверхностных комплексных соединений, которые переходят в раствор с образованием полигетероядерных комплексов. Далее имеет место их полимеризация, в конечном итоге сопровождающаяся формированием первичных частиц (кластеров), которые, укрупняясь, образуют осадок предшественника оксидной системы. Характеристикой процесса анодного растворения является выход по току, который соответствует количеству железа, перешедшего в раствор при определенном текущем значении. Фазовый состав дисперсного продукта, полученного прокаливанием осадка, образовавшегося при низкой концентрации соляной кислоты в электролите при температуре 1100 °С, демонстрирует наличие моно- и гексаферритов бария (99 мас.%). Однако, при повышении концентрации соляной кислоты в электролите в ~6-7 раз преобладающей фазой становится сложный оксид железа (II, III) - 96 мас.%, ферриты бария присутствуют в небольших количествах (~2%). Это указывает на то, что при относительно высоком содержании хлорид-ионов в кислом растворе (pH < 1) основным процессом является исключительно растворение (коррозия) железа. В случае меньших количеств соляной кислоты, скорее всего, возникает конкуренция между нитрат- и хлорид-ионами во время стимулирующей адсорбции, что способствует более равномерному растворению железа и образованию осадка в виде гидроксидов.

Ключевые слова: электрохимический синтез, анодное растворение, низкоуглеродистая сталь, гексаферрит бария, рентгенофазовый анализ

ELECTROCHEMICAL SYNTHESIS OF BARIUM FERRITE PRECURSORS USING RECYCLED INDUSTRIAL IRON

A.F. Dresvyannikov, A.E. Mukhamadeev, A.I. Khairullina, E.E. Valeeva

Alexandr F. Dresvyannikov (ORCID 0000-0002-5824-2307)*, Artur E Mukhamadeev (ORCID 0009-0007-9222-8959), Alina I. Khairullina (ORCID 0000-0003-1683-3894), Elvira E. Valeeva (ORCID 0000-0002-8376-0835)

Department of Electrochemical Technology, Kazan National Research Technological University, Karl Marx st., 68, Kazan, 420015, Russia
E-mail: a.dresvyannikov@mail.ru*, m.artur_98@mail.ru, alina17xaj@mail.ru, elviravaleeva75@yandex.ru

The article demonstrates the feasibility of using anodic oxidation of low-carbon steel to obtain barium ferrites. During the electrolysis, the solution was mixed due to the release of hydrogen at the cathode, and the movement of gas bubbles ensured the movement of electrolyte masses in the direction from the bottom up from the center to the periphery, which facilitates better mixing of electrogenerated reagents (OH^-, Fe^{2+}), electrolyte components and a decrease in concentration polarization. According to modern concepts, the formation of soluble surface complex compounds takes place at the anode, the transition of the latter into solution with the formation of polyheteronuclear complexes, then their polymerization occurs, ultimately accompanied by the formation of primary particles (clusters), which, enlarging, form a precipitate of the oxide system precursor. The characteristic of the anodic dissolution process is the anodic current efficiency, which corresponds to the amount of iron that has passed into solution at a certain current value. The phase composition of the dispersed product obtained by calcining the precipitate formed at a low concentration of hydrochloric acid in the electrolyte at 1100 °C demonstrates the presence of barium mono- and hexaferrites (99% by weight). However, with the hydrochloric acid concentration increase in the electrolyte by ~ 6-7 times, the predominant phase is a complex iron oxide (II, III) in an amount of 96% by weight, barium ferrites are present in small quantities (~ 2%). This indicates that with a relatively high content of chloride ions in an acidic solution (pH < 1), the main process is exclusively the dissolution (corrosion) of iron. In the case of smaller quantities of hydrochloric acid, competition most likely occurs between nitrate and chloride ions during stimulating adsorption, which promotes more uniform dissolution of iron and the formation of a precipitate in the form of hydroxides.

Keywords: electrochemical synthesis, anodic dissolution, low-carbon steel, barium hexaferrite, X-ray phase analysis

Для цитирования:
Дресвянников А.Ф., Мухамадеев А.Э., Хайруллина А.И., Валеева Э.Э. Электрохимический синтез прекурсоров ферритов бария с использованием вторичного технического железа. *Изв. вузов. Химия и хим. технология*. 2025. Т. 68. Вып. 12. С. 74–82. DOI: 10.6060/ivkkt.20256812.7245.

For citation:
Dresvyannikov A.F., Mukhamadeev A.E., Khairullina A.I., Valeeva E.E. Electrochemical synthesis of barium ferrite precursors using recycled industrial iron. *ChemChemTech [Izv. Vyssh. Uchebn. Zaved. Khim. Khim. Tekhnol.]*. 2025. V. 68. N 12. P. 74–82. DOI: 10.6060/ivkkt.20256812.7245.

INTRODUCTION

Currently, the development of resource-saving, energy-efficient, and environmentally friendly technologies for producing competitive products is a priority for science and engineering. In this regard, the issues of rational consumption of industrial raw materials and increasing the efficiency of secondary resource utilization are particularly important. Special attention is given to the development of safe technological processes for the disposal of industrial waste. The main structural material produced in large volumes until now is steel, which defines the material basis of modern civilization.

Metals are non-renewable natural resources, so an important task is to preserve their reserves due to their limited availability. Moreover, metals constitute a significant share of industrial waste, but the issues of their disposal are not always given adequate attention. Such waste has significant material value and can be used to obtain new materials and products with relatively high added value. Thus, worn-out products made of carbon steel, iron scrap, and shavings, which are often difficult to dispose of existing metallurgical methods, are proposed to be used as anode material in the production of iron oxides, including complex oxide systems.

Magnetic materials based on iron oxides are widely used in the production ofdata recording and storage systems, detectors, permanent magnets, and magnetic cooling systems [1]. Much attention is given to the study of iron oxide nanoparticles due to their unique physical and chemical properties, availability, and high technological efficiency in production processes. They have a wide range of applications in the production of biosensors [2], composite polymer materials [3-4], ceramics [5], and magnetic fluids [6-9]. A special place among magnetic materials is occupied by hexagonal M-type ferrites, particularly barium and strontium hexaferrites. As ferrimagnets, they combine

high magnetic susceptibility with semiconductor or dielectric properties, which allows them to dominate the market for new-generation permanent magnets [10], high-density recording media [11], and as absorbing materials in microwave devices and electromagnetic shielding systems [12-13].

Various methods, mainly chemical, are used to obtain dispersed iron oxides and ferrites: precipitation from salt solutions followed by hydrolysis [14-17]; sol-gel technologies [18-19]; thermolysis or thermal decomposition (of hydroxides, nitrates, carbonates, sulphates, chlorides, alcoholates, oxalates, and other iron compounds) [20-21]; solvothermal (hydrothermal) synthesis of ferrites [22-23]. However, chemical processes do not always allow us to obtain oxides with reproducible and controllable properties. Electrochemical methods are also used in the production of ferrites. Electrochemical synthesis is an interesting method to produce crystalline magnetic particles based on quasi-stoichiometric ferrite, in a simple, scalable and water-based way. Electrochemical synthesis was employed to synthesize magnetic nanoparticles of magnetite, and Mn, Ni and Co ferrites [24, 25]. Also cobalt ferrite nanoparticles were prepared, using foils of iron and cobalt as anodes and a counter-electrode of iron as the cathode in 0.04 M n-Bu_4NBr which acts as a surfactant, preventing agglomeration of nanoparticles during synthesis [26]. At [27-28] authors said about synthesis nanodispersed magnetite (Fe_3O_4) with fewer impurities compareding to its natural form. For this the electrochemical method of dissolution of steel sheets or shavings in the heated electrolyte was employed. The advantage of electrochemical synthesis methods is the high purity of the final product, adjustable particle size, and the ability to control the process. A more effective method for obtaining dispersed oxides may be an electrochemical process based on anodic dissolution of electrodes made of iron or low-carbon steel in aqueous solutions of electrolytes with a low content of chloride ions and heat treatment of electrolysis products in the form of precipitate.

This approach is one of the 'soft chemistry' methods, characterized by simpleequipment design, environmental friendliness, and low cost. Electrolysis provides prompt control over process parameters such as electrolyte composition and concentration, anode current density, voltage, etc. It is also used to obtain pure products with reproducible and controllable characteristics, including phase and chemical composition, as well as particle shape and size.

The aim of this work is to study the influence of solution composition and electrolysis mode using a soluble anode made of low-carbon steel on the yield of ferrite phases and to evaluate a possible way of obtaining ferromagnetic materials.

MATERIALS AND METHODS

The electrochemical synthesis of precursors of complex iron-based oxide systems was carried out using the anodic oxidation of an iron (steel) anode, followed by the interaction of iron ions with other electrogenerated reagents and solution components, as well as precipitate separation and high temperature treatment. Electrolysis was performed in a diaphragmless coaxial reactor –electrolyzer using a Mastech DC Power Supply HY3005F-3 power source at room temperature for 1 hour. Carbon steelgrade 3 was used as the anode material (elemental composition: % by weight Fe ~ 98.0%; C – 0.20%; Si – 0.20%; Mn – 0.40%; Ni – 0.2%; Cu – 0.1%; Cr – 0.1%; Co – 0.03%; S – 0.05%; P – 0.04%), and stainless steel grade X18N10T was used as the cathode. Barium nitrate ($Ba(NO_3)_2$, chemically pure, JSC 'LenReactiv') and hydrochloric acid (HCl, chemically pure, JSC 'LenReactiv') were used as the initial components of the electrolyte for barium ferrite synthesis. Characteristics of the electrolysis reactor: the working volume is 175 cm^3; the area of the working electrode (anode) is 40 cm^2; the distance between the electrodes is 3 cm. The electrolysis conditions are presented in Table 1. The electrochemical behavior of the steel anode in the specified electrolyte was studied using polarization curves and chronopotentiograms. The electrode for electrochemical measurements was made of steel grade 3 (iron content – 98.0%), with a fixed working surface area of 1 cm^2. Polarization measurements were carried out using an Elins P-2X potentiostat – galvanostat in a YSE-2 standard electrolysis cell at a temperature of 20±1. Cunder natural aeration conditions in potentiodynamic mode (potential scanning rate: 2 mV/s). A platinum wire electrode was used as the auxiliary electrode and a saturated silver chloride electrode (ELV-1, E = 0.222 V) was used as the reference electrode.

At the end of the process, the precipitate was left to mature in the mother solution for 24 h. It was then separated from the solution by filtration using a Chemker-300 vacuum pump connected to a Bunsen flask. During the filtration process, the precipitate was repeatedly washed with distilled water until allacid residues and ions were completely removed from the solution, which was controlled by indicator paper and a qualitative test for chloride ions. The oxidation rate of the anode was determined by gravimetric method.

The filtered precipitate was dried in a heating cabinet at a temperature of 100 °C. Then it was ground in a mortar to a homogeneous, dispersed state and

weighed. Half of the powder product was calcined in a SNOL 1.4.2.5.1.2/12.5-I1muffle furnace for 2 h at a temperature of 1100 °C.

X-ray phase analysis of the studied samples was performed according to standard methods. The phase composition of the synthesized samples was determined using a D2 PHASER X-ray diffractometer (Bruker) with CoK_α radiation. The identification of crystalline phases was carried out by comparing the obtained experimental values of interplanar distances and relative intensities with the reference values provided in the international PDF-2 database. The quantitative phase composition of the precipitate was calculated using the corundum number method.

Table 1

Electrolysis conditions with soluble steel anode

***Таблица 1.* Условия электролиза с растворимым стальным анодом**

№	Electrolyte composition, mol/l				Current density, mA/cm^2	Synthesis time, h
	$Ba(NO_3)_2$	HCl	pH electrolyte			
			Before electrolysis	After electrolysis		
1	0.35	0.021	1.41	12.75	100	1.0
2		0.14	0.85	11.86		

RESULTS AND DISCUSSION

Preliminary experiments revealed that in barium nitrate solutions, active anodic dissolution of iron does not occur due to the passivation of the electrode surface caused by the formation of an oxide film. This is illustrated by characteristic N-shaped polarization curves featuring a well-defined passivity region (Fig. 1). Therefore, to activate the steel surface, a specific amount of hydrochloric acid solution was added to the electrolyte, which dissociates readily to form chloride ions. When the iron electrode is polarized, intense anodic dissolution is observed, as indicated by the corresponding polarization curves (Fig. 2) and chronopotentiograms (Fig. 3).

The choice of hydrochloric acid as an electrolyte component is based on several factors. Firstly, hydrochloric acid has high electrical conductivity due to the relay mechanism of proton transfer. Secondly, its use promotes the dissolution of the anode not only

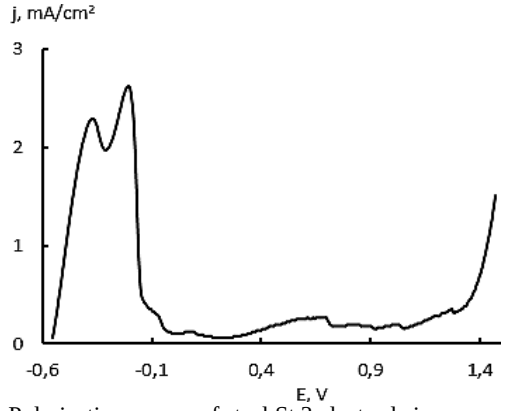

Fig. 1. Polarization curves of steel St.3 electrode in aqueous solution of barium nitrate 0.35 M $Ba(NO_3)_2$

Рис. 1. Поляризационные кривые стального (Ст. 3) электрода в водном растворе нитрата бария 0,35 М $Ba(NO_3)_2$

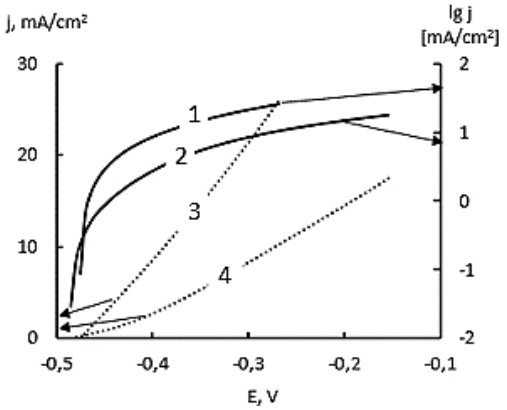

Fig. 2. Polarization curves of steel electrode St.3 in aqueous solution of the composition: 1, 3 - 0.35 M $Ba(NO_3)_2$+0.14M HCl; 2, 4 - 0.35 M $Ba(NO_3)_2$+0.02 M HCl

Рис. 2. Поляризационные кривые стального электрода Ст.3 в водном растворе состава: 1, 3 – 0,35 М $Ba(NO_3)_2$+0,14М HCl; 2, 4 – 0,35 М $Ba(NO_3)_2$+0,02 М HCl

electrochemically, but also chemically, allowing iron to be ionized rapidly. Barium nitrate was selected as the barium salt because of its good solubility in water and the sufficiently high electrical conductivity of the solution. Additionally, barium nitrate is often considered an industrial waste from various technological processes [29] and can potentially be used for the production of ferrites through electrochemical methods.

The concentration of barium nitrate in the electrolyte was increased to 0.35 mol/l, as this represents the maximum solubility of the salt and the highest conductivity of its aqueous solution (approximately 35 mS/cm).

By analyzing the anodic polarization curves of St. 3 in the corresponding solutions, we can conclude that, as mentioned above, the curve of the single-component solution of barium nitrate (Fig. 1) exhibits a shape characteristic of passivating metals. The region

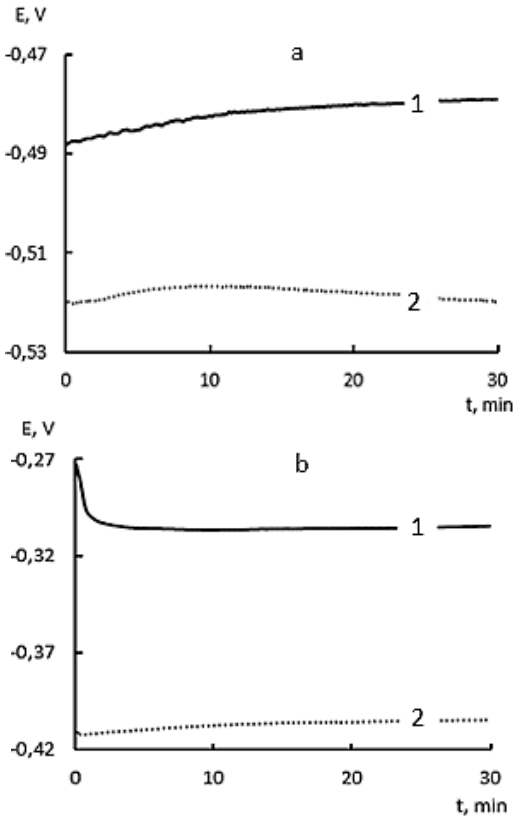

Fig. 3. Chronopotentiograms of steel electrode (St.3) under open circuit conditions (a) and anodic galvanostatic polarization (b, i=20 mA/sm^2, 30 min) in solution of the following composition: 1 – 0.35M $Ba(NO_3)_2$+0.14M HCl; 2 – 0.35M $Ba(NO_3)_2$+0.02 M HCl

Рис. 3. Хронопотенциограммы стального электрода (Ст.3) в условиях разомкнутой цепи (а) и анодной гальваностатической поляризации (b, i=20 мА/см^2, 30 мин) в растворе состава: 1 – 0,35М $Ba(NO_3)_2$+0,14М HCl; 2 – 0,35М $Ba(NO_3)_2$+0,02М HCl

of active dissolution (or active-passive transitions), where an anodic current maximum occurs, and the regions of passive state and transpassivity are clearly observed. When acid is added, active dissolution of the metal occurs, and the rate of steel dissolution varies with different acid concentrations (Fig. 2). With lower acid concentrations, there is greater polarization of the electrode, which results in the formation of soluble surface complexes and their transition into solution [30].

At high acid concentrations (> 0.1 M) under open-circuit conditions (Fig. 3, a, curve 1), the metal potential shifts monotonically towards more positive values, indicating a slow down in the corrosion process. Despite the high concentration of chloride ions, the electrode becomes passivated gradually, likely due to the formation of poorly soluble surface oxide-hydroxide films. However, at lower acid concentrations (Fig. 3a, curve 2), the electrode potential initially shifts towards more positive values and then shifts back. This behavior may indicate the mutual adsorption of nitrate and chloride ions along with water molecules on the electrode surface, leading to their competition in the passivation-activation processes of the steel. During the galvanostatic anodic polarization of the electrode in a solution with with high acid content (Fig. 3b, curve 1), the steady-state potential shifts into the anodic region by 0.22 V, then after 5-7 minutes, it sharply shifts towards more negative values and remains relatively unchanged throughout the entire process. In a solution with a smaller amount of acid (Fig. 3b, curve 2), the steady-state potential shifts gradually towards the anodic region.

There gularities in the behavior of steel electrodes, mentioned above, were taken into account during the electrolysis process. The process was conducted in a coaxial reactor-electrolyzer with an anode current density of 100 mA/cm² for a duration of 1 hour. During the electrolysis, the solution was heated and stirred by the release of hydrogen at the cathode. The movement of gas bubbles caused the electrolyte masses to move in a bottom-up direction from the center to the periphery, which contributed to better mixing of the electrogenerated reagents (OH^- , Fe^{2+}) and electrolyte components as well as reducing the concentration of polarization. According to modern concepts, soluble surface complexes form at the anode, entering the solution and forming polyheteronuclear complexes. Their polymerization then occurs, eventually leading to the formation of primary particles (clusters) [31], which grow to form the precursor precipitate of the oxide system.

The characteristic of the anodic dissolution process is the anodic current efficiency, which records the amount of iron transferred in to the solution at a given current value (Table 2). After the electrolysis was completed and the precipitate was allowed to mature in the electrolyte for 24 h, it was separated from the mother solution. The precipitate was then treated as described above and calcined at 1100 °C. The phase composition of the dispersed product obtained by calcination of the precipitate formed at a low concentration of hydrochloric acid (0.021 M; Table 3, sample 1) in the electrolyte shows the presence of barium mono- and hexaferrites. However, a 6- to 7-fold increase in the concentration of hydrochloric acid in the electrolyte results in an increase in the amount of complex iron oxide (II, III) to 96% by weight, making it the predominant phase, while barium ferrite is present in small amounts (~ 2%). This indicates that at relatively high concentrations of chloride ions in acidic solution (pH < 1), the main process is exclusively the dissolution (corrosion) of iron. In the case of small amounts

of hydrochloric acid, it is most likely that there is competition between nitrate and chloride ions in stimulating adsorption, which promotes more uniform dissolution of iron and the formation of a precipitate in the form of precursors of oxide systems.

Fig. 4 shows the X-ray diffraction patterns of the precipitation samples that were calcined at 1100 °C. The diffraction pattern (Fig. 4, Table 3) of sample 1 indicates the predominance of barium hexaferrite (76%) with a hexagonal structure and barium monoferrite (23%) with an orthorhombic structure in its phase composition, along with an extremely small amount of iron oxide (II, III) – approximately 1%. In sample 2, obtained from electrolyte with an increased concentration of hydrochloric acid and calcined at 1100 °C, barium ferrites are formed in small quantities (approximately 2%), while the predominant phase of the dispersed product is iron oxide (II, III).

Table 2

Estimation of the oxidation rate of the steel anode and the current efficiency in $Ba(NO_3)_2$ + HCl solutions

***Таблица 2.* Оценка скорости окисления стального анода и выход по току в растворах $Ba(NO_3)_2$ + HCl**

№	Composition of solutions	j, mA/cm^2	Oxidation rate, mg/cm^2·h	Current outputa, %
1	0,35M $Ba(NO_3)_2$ + + 0,021 M HCl	100	35	34
2	0,35M $Ba(NO_3)_2$ + + 0,14 M HCl		72	69

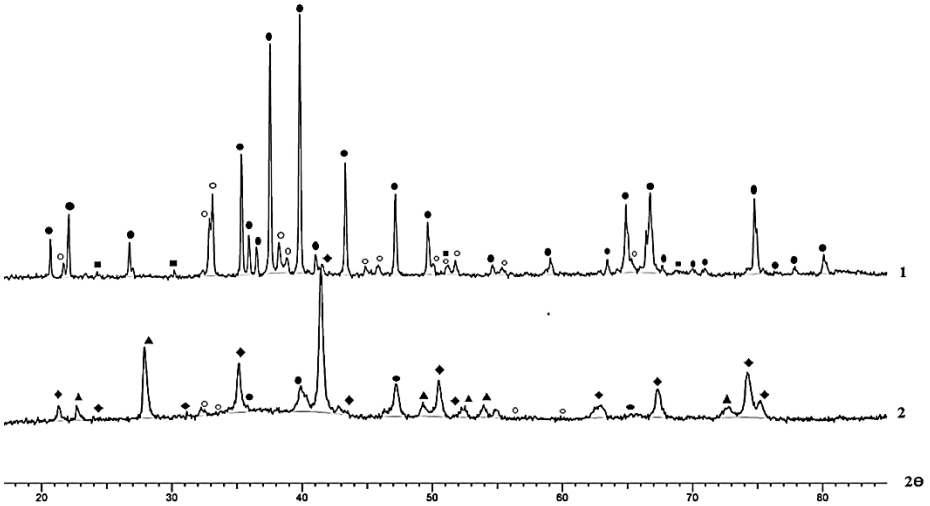

Fig. 4. X-ray diffraction patterns of the studied samples calcined at 1100 ºC. The curve numbers correspond to the experiment numbers in Tables 1, 2

Рис. 4. Рентгеновские дифрактограммы исследуемых образцов, прокаленных при 1100 °C; Номера кривых соответствуют номерам экспериментов в табл. 1, 2

Table 3

Results of X-ray phase analysis of heat-treated samples

***Таблица 3*. Результаты рентгенофазового анализа термобработанных образцов**

№	Phase composition	Content, %	Coherent scattering region, nm	Spacegroup	Crystal lattice type (syngony)	Unit cell parameters			
						a	B	c	z
1	$BaFe_{12}O_{19}$	76	66	P63/mmc (194)	Hexagonal	8.893	-	23.19	-
	$BaFe_2O_4$	23	29	Bb21m(36)	Orthorhombic	18.99	5.38	8.44	8
	Fe_2O_3	1	-	P41 31(213)	Cubic	8.33	-	-	-
2	Fe_3O_4	96	35	P12/c1(13)	Monoclinic	5.94	5.92	16.77	8
	$Ba_2Fe_{30}O_{46}$	2	40	R-3m(166)	Hexagonal	5.88	-	84.11	3
	$BaFe_{12}O_{19}$	2	41	P63/mmc (194)	Hexagonal	5.89	-	23.18	2
	Ba_2FeO_4	<1	-	P12/n1(14)	Monoclinic	6.03	7.65	10.16	4

CONCLUSIONS

The influence of solution composition and electrolysis mode on the production of barium ferrite using the anodic dissolution of low-carbon steel in a coaxial diaphragmless reactor-electrolyzer, followed by the heat treatment of the formed precipitates, was investigated.

It was found that to achieve the highest yield of barium ferrites, particularly barium hexaferrite, it is

necessary to adjust the concentration of HCl in the electrolyte to values below 0.025 M.

It was revealed that an important factor in the synthesis of barium ferrites is a change in the acidity of the electrolyte during the electrolysis process, which promotes the formation of precipitates in the form of oxo-hydroxo compounds of iron and barium.

The experiments demonstrated that heat treatment at 1100 °C of the precipitate obtained using an electrolyte of 0.35 M $Ba(NO_3)_2$ + 0.021 M HCl in a coaxial reactor-electrolyzer at anode current density of 100 mA/cm² results in a dispersed product consisting of barium hexaferrite (76%) with a hexagonal structure and barium monoferrite (23%) with an orthorhombic structure, with minimal impurities.

ACKNOWLEDGEMENT

The work was carried out with the financial support of the Ministry of Science and Higher Education of the Russian Federation within the framework of the state assignment for the provision of public services (performance of works) dated December 29, 2022, No. 075-01508-23-00. The research topic is "Creating scientific foundations for the production of new multifunctional materials with a wide range of applications" (FZSG-2023-0008).

Работа выполнена при финансовой поддержке Министерства науки и высшего образования Российской Федерации в рамках государственного задания на оказание государственных услуг (выполнение работ) от 29.12.2022 г. № 075-01508-23-00. Тема исследования «Создание научных основ получения новых мультифункциональных материалов широкого спектра применения» (FZSG-2023-0008).

КОНФЛИКТ ИНТЕРЕСОВ

Авторы заявляют об отсутствии конфликта интересов, требующего раскрытия в данной статье.

The authors declare the absence of a conflict of interest warranting disclosure in this article.

ЛИТЕРАТУРА

1. **Shull R.D.** Magnetocaloric effect of ferromagnetic particles. *IEEE Trans. Mag.* 1993. V. 29. P. 2614-2615. DOI: 10.1109/20.280849.
2. **Губин С.П., Кокшаров Ю.А., Хомутов Г.Б., Юрков Г.Ю.** Магнитные наночастицы: методы получения, строение и свойства. *Усп. химии*. 2005. Т. 74. № 6. С. 539-574. DOI: 10.1070/RC2005v074n06ABEH000897.
3. **Balars A.C., Emrick T., Russel T.P.** Nanoparticle Polymer Composites: Where Two Small Worlds Meets. *Science*. 2006. V. 314. P. 1107-1110. DOI: 10.1126/science.1130557.
4. **Ditsch A., Laibinis P.E., Wang D.I.C., Hatton T.A.** Controlled Clustering and Enhanced Stability of Polymer-Coated Magnetic Nanoparticles. *Langmuir*. 2005. V. 21. P. 6006-6018. DOI: 10.1021/la047057.
5. **Лысенко В.И., Горев В.Н., Литвиненко Ю.А., Бардаханов С.П.** Получение и свойства керамики из нанопорошка оксида железа. *Вестн. НГУ. Сер.: Физика*. 2013. Т. 8. № 1. С. 99-103. DOI: 10.54362/1818-7919-2013-8-1-99-103.
6. **Такетоми С., Тикадзуми С.** Магнитные жидкости. М.: Мир. 1993. 272 с.
7. **Chen K., Bakusis A.F., Luo W.** Improving surfactant grafting in magnetic colloids. *Appl. Surf. Sci.* 2006. V. 252. P. 6379-6382. DOI: 10.1016/j.apsusc.2005.12.160.
8. **Ge J., Biasini M., Dong C., Guo J., Beyermann W.P.** One step-synthesis of Highly Water-Soluble Magnetic Colloidal Nanocrystals. *Chem. Eur. J.* 2007. V. 13. P. 7153-7161. DOI: 10.1002/chem.200700375.
9. **Hong R.Y., Pan T.T., Han Y.P., Li H.Z., Ding J., Han S.** Magnetic field synthesis of Fe_3O_4 nanoparticles used as precursor of ferrofluids. *JMMM*. 2007. V.310. P. 37-47. DOI: 10.1016/j.jmmm.2006.07.026.
10. **Канева И.И., Костишин В.Г., Андреев В.Г., Читанов Д.Н., Николаев А.Н., Кислякова Е.И.** Получение гексаферрита бария с повышенными изотропными свойствами.

REFERENCES

1. **Shull R.D.** Magnetocaloric effect of ferromagnetic particles. *IEEE Trans. Mag.* 1993. V. 29. P. 2614-2615. DOI: 10.1109/20.280849.
2. **Gubin S.P., Koksharov Yu.A., Khomutov G.B., Yurkov G.Yu.** Magnetic nanoparticles: preparation, structure and properties. *Russ. Chem. Rev.* 2005. V. 74. N 6. P. 489-520. DOI: 10.1070/RC2005v074n06ABEH000897.
3. **Balars A.C., Emrick T., Russel T.P.** Nanoparticle Polymer Composites: Where Two Small Worlds Meets. *Science*. 2006. V. 314. P. 1107-1110. DOI: 10.1126/science.1130557.
4. **Ditsch A., Laibinis P.E., Wang D.I.C., Hatton T.A.** Controlled Clustering and Enhanced Stability of Polymer-Coated Magnetic Nanoparticles. *Langmuir*. 2005. V. 21. P. 6006-6018. DOI: 10.1021/la047057.
5. **Lysenko V.I., Gorev V.N., Litvinenko Yu.A., Bardakhanov S.P.** Production and properties of ceramics from iron oxide nanopowder. *Vestn. NGU. Ser: Fizika.* 2013. V. 8. N 1. P. 99-103 (in Russian). DOI: 10.54362/1818-7919-2013-8-1-99-103.
6. **Taketomi S., Chikazumi S.** Magnetic fluids. M.: Mir. 1993. 272 p. (in Russian).
7. **Chen K., Bakusis A.F., Luo W.** Improving surfactant grafting in magnetic colloids. *Appl. Surf. Sci.* 2006. V. 252. P. 6379-6382. DOI: 10.1016/j.apsusc.2005.12.160.
8. **Ge J., Biasini M., Dong C., Guo J., Beyermann W.P.** One step-synthesis of Highly Water-Soluble Magnetic Colloidal Nanocrystals. *Chem. Eur. J.* 2007. V. 13. P. 7153-7161. DOI: 10.1002/chem.200700375.
9. **Hong R.Y., Pan T.T., Han Y.P., Li H.Z., Ding J., Han S.** Magnetic field synthesis of Fe_3O_4 nanoparticles used as precursor of ferrofluids. *JMMM*. 2007. V. 310. P. 37-47. DOI: 10.1016/j.jmmm.2006.07.026.
10. **Kaneva I.I., Kostishin V.G., Andreev V.G., Chitanov D.N., Nikolaev A.N., Kislyakova E.I.** Production of barium hexaferrite with improved isotropic properties. *Izv. VUZov.*

Изв. вузов. Матер. электрон. техники. 2014. Т. 17. № 3. С. 183-188. DOI: 10.17073/1609–3577–2014–3–183–188.

11. **Martirosyan K., Galstyan E., Hossain S., Wang Y.-J., Litvinov D.** Barium hexaferrite nanoparticles: synthesis and magnetic properties. *Mater. Sci. Eng., B.* 2011. V. 176. N 1. P. 8-13. DOI: 10.1016/j.mseb.2010.08.005.
12. **Harris V.G., Chen Z., Chen Y., Yoon S., Sakai T., Gieler A., Yang A., He Y., Ziemer K.S., Sun N.X., Vittoria C.** Ba-hexaferrite films for next generation microwave devices (invited). *J. Appl. Phys.* 2006. V. 99. N 8. P. 08M911-1-08M911-5. DOI: 10.1063/1.2165145.
13. **Ghasemi A., Hossienpour A., MorisakoA., Liu X., Ashrafizadeh A.** Investigation of the microwave absorptive behavior of doped barium ferrites. *Mater. Des.* 2008. V. 29. N 1. P. 112-117. DOI: 10.1016/j.matdes.2006.11.019.
14. **Pankhurst Q.A., Connolly J., Jones S., Dobson J.** Applications of magnetic nanoparticles in biomedicine. *J. Phys. D: Appl. Phys.* 2003. V. 36. N 13. P. R167 - R181. DOI: 10.20538/1682-0363-2008-2-70-78.
15. **Veverka P., Pollert E., Zaveta K., Vasseur S., Duguet E.** Sr-hexaferrrite/maghemite composite nanoparticles – possible new mediators for magnetic hyperthermia. *J. Nannotech.* 2008. V. 19. N 21. P. 215705. DOI: 10.1088/0957-4484/19/21/215705.
16. **Hyeon T.** Chemical Synthesis of Magnetic Nanoparticles. *Chem. Commun.* 2003. P. 927-934. DOI: 10.1039/B207789B.
17. **Балмасова О.В., Королев В.В., Ефимова К.В.** Магнитотепловые свойства феррита меди. *Изв. вузов. Химия и хим. технология.* 2024. Т. 67. Вып. 1. С. 45-50. DOI: 10.6060/ivkkt.20246701.6851.
18. **Martinez-Mera I., Espinoza-Pesqueira M.E., Perez-Hernandez R., Arenas-Alatorre J.** Synthesis of magnetite (Fe_3O_4) nanoparticles withour surfactants at room temperature. *Mater. Lett.* 2007. V. 61. P. 927-934. DOI: 10.1016/j.matlet.2007.02.018.
19. **Junliang L., Ping L., Xingkai Z., Dongjun P., Peng Z., Ming Z.** Synthesis and properties of single domain sphere-shaped barium hexa-ferrite nano powders via an ultrasonic-assisted co-precipitation route. *Ultrason. Sonochem.* 2015. V. 23. P. 46-52. DOI: 10.1016/j.ultsonch.2014.08.001.
20. **Liu X., Kaminski M.D., Guan Y., Chen H., Liu H., Rosengart A.J.** Preparation and characterization of hydrophobic superparamagnetic magnetite gel. *JMMM.* 2006. V. 306. P. 248–253.
21. **Meng Y.Y., He M.H., Zeng Q., Jiao D.L., Shukla S., Ramanujan R.V., Liu Z.W.** Synthesis of barium ferrite ultrafine powders by a sol-gel combustion method using glycine gels. *J. Alloys Compd.* 2014. V. 583. P. 220-225. DOI: 10.1016/j.jallcom.2013.08.156. DOI: 10.1016/j.jmmm.2006.03.049.
22. **Park J., Lee E., Hwang N.-M., Kang M.,Kim S.C., Hwang Y., Park J.-G., Noh H.-J., Kim J.-Y., Park J.-H., Hyeon T.** One-Nanometer-Scale Size-Controlled Synthesis of Monodisperse Magnetic Iron Oxide Nanoparticles. *Angew. Chem. Int. Ed.* 2005. V. 44. P. 2872–2877. DOI: 10.1002/anie.200461665.
23. **Peng S., Wang C., Xie J., Sun S.** Synthesis and stabilization of monodisperse Fe nanoparticles. *J. Am. Chem. Soc.* 2006. V. 128. P. 10676–1067. DOI: 10.1021/ja063969h.
24. **Ovejero J.G., Mayoral A., Cañete M., García M., Hernando A., Herrasti P.** Electrochemical Synthesis and Magnetic Properties of MFe2O4 (M = Fe, Mn, Co, Ni) Nanoparticles for Potential Biomedical Applications. *J. Nanosci. Nanotechnol.* 2019. 19. P. 2008–2015. DOI: 10.1166/jnn.2019.15313.
25. **Ritter T.G., Phakatkar A.H., Md Golam Rasul, Tolou Shokuhfar, Gonçalves J.M., Shahbazian-Yassar R.** Electrochemical synthesis of high entropy hydroxides and oxides

Meter. Elektron. Tekh. 2014. V.17. N 3. P. 183-188 (in Russian). DOI: 10.17073/1609–3577–2014–3–183–188.

11. **Martirosyan K., Galstyan E., Hossain S., Wang Y.-J., Litvinov D.** Barium hexaferrite nanoparticles: synthesis and magnetic properties. *Mater. Sci. Eng., B.* 2011. V. 176. N 1. P. 8-13. DOI: 10.1016/j.mseb.2010.08.005.
12. **Harris V.G., Chen Z., Chen Y., Yoon S., Sakai T., Gieler A., Yang A., He Y., Ziemer K.S., Sun N.X., Vittoria C.** Ba-hexaferrite films for next generation microwave devices (invited). *J. Appl. Phys.* 2006. V. 99. N 8. P. 08M911-1-08M911-5. DOI: 10.1063/1.2165145.
13. **Ghasemi A., Hossienpour A., MorisakoA., Liu X., Ashrafizadeh A.** Investigation of the microwave absorptive behavior of doped barium ferrites. *Mater. Des.* 2008. V. 29. N 1. P. 112-117. DOI: 10.1016/j.matdes.2006.11.019.
14. **Pankhurst Q.A., Connolly J., Jones S., Dobson J.** Applications of magnetic nanoparticles in biomedicine. *J. Phys. D: Appl. Phys.* 2003. V. 36. N 13. P. R167 - R181. DOI: 10.20538/1682-0363-2008-2-70-78.
15. **Veverka P., Pollert E., Zaveta K., Vasseur S., Duguet E.** Sr-hexaferrrite/maghemite composite nanoparticles – possible new mediators for magnetic hyperthermia. *J. Nannotech.* 2008. V. 19. N 21. P. 215705. DOI: 10.1088/0957-4484/19/21/215705.
16. **Hyeon T.** Chemical Synthesis of Magnetic Nanoparticles. *Chem. Commun.* 2003. V. 21. N 8. P. 927-934. DOI: 10.1039/B207789B.
17. **Balmasova O.V., Korolev V.V., Efimova K.V.** Magnetothermal properties of copper ferrite. *ChemChemTech [Izv. Vyssh. Uchebn. Zaved. Khim. Khim. Tekhnol.]*. 2024. V. 67. N 1. P. 45-50. DOI: 10.6060/ivkkt.20246701.6851.
18. **Martinez-Mera I., Espinoza-Pesqueira M.E., Perez-Hernandez R., Arenas-Alatorre J.** Synthesis of magnetite (Fe_3O_4) nanoparticles withour surfactants at room temperature. *Mater. Lett.* 2007. V. 61. P. 927-934. DOI: 10.1016/j.matlet.2007.02.018.
19. **Junliang L., Ping L., Xingkai Z., Dongjun P., Peng Z., Ming Z.** Synthesis and properties of single domain sphere-shaped barium hexa-ferrite nano powders via an ultrasonic-assisted co-precipitation route. *Ultrason. Sonochem.* 2015. V. 23. P. 46-52. DOI: 10.1016/j.ultsonch.2014.08.001.
20. **Liu X., Kaminski M.D., Guan Y., Chen H., Liu H., Rosengart A.J.** Preparation and characterization of hydrophobic superparamagnetic magnetite gel. *JMMM.* 2006. V. 306. P. 248–253.
21. **Meng Y.Y., He M.H., Zeng Q., Jiao D.L., Shukla S., Ramanujan R.V., Liu Z.W.** Synthesis of barium ferrite ultrafine powders by a sol-gel combustion method using glycine gels. *J. Alloys Compd.* 2014. V. 583. P. 220-225. DOI: 10.1016/j.jallcom.2013.08.156. DOI: 10.1016/j.jmmm.2006.03.049.
22. **Park J., Lee E., Hwang N.-M., Kang M.,Kim S.C., Hwang Y., Park J.-G., Noh H.-J., Kim J.-Y., Park J.-H., Hyeon T.** One-Nanometer-Scale Size-Controlled Synthesis of Monodisperse Magnetic Iron Oxide Nanoparticles. *Angew. Chem. Int. Ed.* 2005. V. 44. P. 2872–2877. DOI: 10.1002/anie.200461665.
23. **Peng S., Wang C., Xie J., Sun S.** Synthesis and stabilization of monodisperse Fe nanoparticles. *J. Am. Chem. Soc.* 2006. V. 128. P. 10676–1067. DOI: 10.1021/ja063969h.
24. **Ovejero J.G., Mayoral A., Cañete M., García M., Hernando A., Herrasti P.** Electrochemical Synthesis and Magnetic Properties of MFe2O4 (M = Fe, Mn, Co, Ni) Nanoparticles for Potential Biomedical Applications. *J. Nanosci. Nanotechnol.* 2019. 19. P. 2008–2015. DOI: 10.1166/jnn.2019.15313.

boosted by hydrogen evolution reaction. *Cell Rep. Phys. Sci.* 2022. V. 3. P. 100847. DOI: 10.1016/j.xcrp.2022.100847.
26. **Mazar E., Herrasti P., Morales M.P., Menendez N.** Synthesis and characterization of CoFe2O4 ferrite nanoparticles obtained by an electrochemical method. *Nanotechnology*. 2012. V. 23. P. 355708. DOI: 10.1088/0957-4484/23/35/355708.
27. **Kalaeva S.Z., Yamanina N.S., Makaro V.M. Zaharova I.N., Shipilin A.M., Solovyova A.N., Terzi M.E.** The synthesis of nanodispersed magnetite using electrochemical method. *J. Nano-Electron. Phys.* 2014. V. 6. N 3. P. 03030.
28. **Григорьева И.О., Дресвянников А.Ф.** Электрохимический синтез дисперсного феррита бария с использованием анодного растворения металла. *Изв. вузов. Химия и хим. технология.* 2021. Т. 64. Вып. 4. С. 59-66. DOI: 10.6060/ivkkt.20216404.6315.
29. **Samouhos M., Taxiarchou M.** D4.3 Circular Economy and zero waste aspects and business models of production. URL: http://scrreen.eu/wpcontent/uploads/2018/07/D4.3-Circular-Economy-and-zero-waste-aspects-and-business-modelsof-production.
30. **Yamauchi T., Tsukahara Y., Sakata T., Mori H., Chikata T., Katoh S., Wada Y.** Barium ferrite powders prepared by microwave-induced hydrothermal reaction and magnetic property. *J. Magn. Magn. Mater.* 2009. V. 321. N 1. P. 8-11. DOI: 10.1016/j.jmmm.2008.07.005.
31. **Liu Y., Drew M.G.B., Liu Y., Wang J., Zhang M.** Efficiency and purity control in the preparation of pure and/or aluminum-doped barium ferrites by hydrothermal methods using ferrous ions as reactants. *J. Magn. Magn. Mater.* 2010. V. 322. N 3. P. 366-374. DOI: 10.1016/j.jmmm.2009.09.062.

25. **Ritter T.G., Phakatkar A.H., Md Golam Rasul, Tolou Shokuhfar, Gonçalves J.M., Shahbazian-Yassar R.** Electrochemical synthesis of high entropy hydroxides and oxides boosted by hydrogen evolution reaction. *Cell Rep. Phys. Sci.* 2022. V. 3. P. 100847. DOI: 10.1016/j.xcrp.2022.100847.
26. **Mazar E., Herrasti P., Morales M.P., Menendez N.** Synthesis and characterization of CoFe2O4 ferrite nanoparticles obtained by an electrochemical method. *Nanotechnology*. 2012. V. 23. P. 355708. DOI: 10.1088/0957-4484/23/35/355708.
27. **Kalaeva S.Z., Yamanina N.S., Makaro V.M. Zaharova I.N., Shipilin A.M., Solovyova A.N., Terzi M.E.** The synthesis of nanodispersed magnetite using electrochemical method. *J. Nano-Electron. Phys.* 2014. V. 6. N 3. P. 03030.
28. **Grigoryeva I.O., Dresvyannikov A.F.** Electrochemical synthesis of dispersed barium ferrite using anodic dissolution of metal. *ChemChemTech [Izv. Vyssh. Uchebn. Zaved. Khim. Khim. Tekhnol.]*. 2021. V. 64. N 4. P. 59-66 (in Russian). DOI: 10.6060/ivkkt.20216404.6315.
29. **Samouhos M., Taxiarchou M.** D4.3 Circular Economy and zero waste aspects and business models of production. URL: http://scrreen.eu/wpcontent/uploads/2018/07/D4.3-Circular-Economy-and-zero-waste-aspects-and-business-modelsof-production.
30. **Yamauchi T., Tsukahara Y., Sakata T., Mori H., Chikata T., Katoh S., Wada Y.** Barium ferrite powders prepared by microwave-induced hydrothermal reaction and magnetic property. *J. Magn. Magn. Mater.* 2009. V. 321. N 1. P. 8-11. DOI: 10.1016/j.jmmm.2008.07.005.
31. **Liu Y., Drew M.G.B., Liu Y., Wang J., Zhang M.** Efficiency and purity control in the preparation of pure and/or aluminum-doped barium ferrites by hydrothermal methods using ferrous ions as reactants. *J. Magn. Magn. Mater.* 2010. V. 322. N 3. P. 366-374. DOI: 10.1016/j.jmmm.2009.09.062.

Поступила в редакцию 21.03.2025
Принята к опубликованию 06.06.2025

Received 21.03.2025
Accepted 06.06.2025